T2 Mapping from Super-Resolution-Reconstructed Clinical Fast Spin Echo Magnetic Resonance Acquisitions

Hélène Lajous[1,2], Tom Hilbert[1,3,4], Christopher W. Roy[1], Sébastien Tourbier[1], Priscille de Dumast[1,2], Thomas Yu[4], Jean-Philippe Thiran[1,4], Jean-Baptiste Ledoux[1,2], Davide Piccini[1,3], Patric Hagmann[1], Reto Meuli[1], Tobias Kober[1,3,4], Matthias Stuber[1,2], Ruud B. van Heeswijk[1], and Meritxell Bach Cuadra[1,2,4]

[1] Department of Radiology, Lausanne University Hospital (CHUV) and University of Lausanne (UNIL), Lausanne, Switzerland
helene.lajous@unil.ch
[2] Center for Biomedical Imaging (CIBM), Lausanne, Switzerland
[3] Advanced Clinical Imaging Technology (ACIT), Siemens Healthcare, Lausanne, Switzerland
[4] Signal Processing Laboratory 5 (LTS5), Ecole Polytechnique Fédérale de Lausanne (EPFL), Lausanne, Switzerland

Abstract. Relaxometry studies in preterm and at-term newborns have provided insight into brain microstructure, thus opening new avenues for studying normal brain development and supporting diagnosis in equivocal neurological situations. However, such quantitative techniques require long acquisition times and therefore cannot be straightforwardly translated to *in utero* brain developmental studies. In clinical fetal brain MRI routine, 2D low-resolution T2-weighted fast spin echo sequences are used to minimize the effects of unpredictable fetal motion during acquisition. As super-resolution techniques make it possible to reconstruct a 3D high-resolution volume of the fetal brain from clinical low-resolution images, their combination with quantitative acquisition schemes could provide fast and accurate T2 measurements. In this context, the present work demonstrates the feasibility of using super-resolution reconstruction from conventional T2-weighted fast spin echo sequences for 3D isotropic T2 mapping. A quantitative MR phantom was imaged using a clinical T2-weighted fast spin echo sequence at variable echo time to allow for super-resolution reconstruction at every echo time and subsequent T2 mapping of samples whose relaxometric properties are close to those of fetal brain tissue. We demonstrate that this approach is highly repeatable, accurate and robust when using 6 echo times (total acquisition time less than 9 minutes) as compared to gold-standard single-echo spin echo sequences (on the order of several hours for one single 2D slice).

Keywords: Super-Resolution (SR) reconstruction · T2 mapping · T2-weighted images · Fast spin echo sequences · Fetal brain MRI.

1 Introduction

Early brain development encompasses many crucial structural and physiological modifications that have an influence on health later in life. Changes in T1 and T2 relaxation times may provide valuable clinical information about ongoing biological processes, as well as a better insight into the early stages of normal maturation [5]. Indeed, quantitative MRI (qMRI) has revealed biomarkers sensitive to subtle changes in brain microstructure that are characteristic of abnormal patterns and developmental schemes in newborns [20, 6]. T1 and T2 mapping of the developing fetal brain would afford physicians new resources for pregnancy monitoring, including quantitative diagnostic support in equivocal situations and prenatal counselling, as well as postnatal management. Unfortunately, current relaxometry strategies require long scanning times that are not feasible in the context of *in utero* fetal brain MRI due to unpredictable fetal motion in the womb [15, 4, 23, 8]. As such, very little work has explored *in vivo* qMRI of the developing fetal brain. Myelination was characterized *in utero* using a monopoint T1 mapping based on fast spoiled gradient echo acquisitions [1], and more recently by fast macromolecular proton fraction mapping [25]. T2* relaxometry of the fetal brain has been explored through fast single-shot multi-echo gradient echo-type echo-planar imaging (GRE-EPI) [24] and, recently, based on a slice-to-volume registration of 2D dual-echo multi-slice EPI with multiple time points reconstructed into a motion-free isotropic high-resolution (HR) volume [3]. To our knowledge, similar strategies have not been investigated for *in utero* T2 mapping yet. Today, super-resolution (SR) techniques have been adopted to take advantage of the redundancy between multiple T2-weighted (T2w) low-resolution (LR) series acquired in orthogonal orientations to reconstruct a single isotropic HR volume of the fetal brain with reduced motion sensitivity for thorough anatomical exploration [9, 19, 11, 22, 7]. In clinical routine, 2D thick slices are typically acquired in a few seconds using T2w multi-slice single-shot fast spin echo sequences [8]. We hypothesize that the combination of SR fetal brain MRI with the sensitivity of qMRI would enable robust and reliable 3D HR T2 relaxometry of the fetal brain [3, 2]. In this context, we have explored the feasibility of repeatable, accurate and robust 3D HR T2 mapping from SR-reconstructed clinical fast T2w Half-Fourier Acquisition Single-shot Turbo spin Echo (HASTE) with variable echo time (TE) on a quantitative MR phantom [12].

2 Methodology

2.1 Model fitting for T2 mapping

The T2w contrast of an MR image is governed by an exponential signal decay characterized by the tissue-specific relaxation parameter, T2. Since any voxel within the brain tissue may contain multiple components, a multi-exponential model is the closest to reality. However, it requires long acquisition times that are not acceptable in a fetal context. The common simplification of a single-compartment model [6, 15] allows for fitting the signal according to the following

equation:

$$\hat{X}_{\mathrm{TE}} = \mathcal{M}_0 e^{\frac{-TE}{T2}}, \tag{1}$$

where $\mathcal{M}_0$ is the equilibrium magnetization and $\hat{X}_{\mathrm{TE}}$ is the signal intensity at a given echo time TE at which the image is acquired. As illustrated in Figure 1, the time constant T2 can be estimated in every voxel by fitting the signal decay over TE with this mono-exponential analytical model [17].

We aim at estimating a HR 3D T2 map of the fetal brain with a prototype algorithm. Our strategy is based on SR reconstruction from orthogonal 2D multi-slice T2w clinical series acquired at variable TE (see complete framework in Figure 1). For every TE_i, a motion-free 3D image $\hat{\mathbf{X}}_{TE_i}$ is reconstructed using a Total-Variation (TV) SR reconstruction algorithm [22, 21] which solves:

$$\hat{\mathbf{X}}_{TE_i} = \arg\min_{\mathbf{X}} \frac{\lambda}{2} \sum_{kl} \| \underbrace{\mathbf{D}_{kl}\mathbf{B}_{kl}\mathbf{M}_{kl}}_{\mathbf{H}_{kl}} \mathbf{X} - \mathbf{X}^{LR}_{kl,TE_i} \|^2 + \|\mathbf{X}\|_{TV}, \tag{2}$$

where the first term relates to data fidelity, k being the k-th LR series $\mathbf{X}^{LR}_{TE_i}$ and l the l-th slice. $\|\mathbf{X}\|_{TV}$ is a TV prior introduced to regularize the solution while λ balances the trade-off between both data and regularization (λ=0.75). $\mathbf{D}$ and $\mathbf{B}$ are linear downsampling and Gaussian blurring operators given by the acquisition characteristics. $\mathbf{M}$, which encodes the rigid motion of slices, is set to the identity transform in the absence of motion.

The model fitting described in Equation 1 is computed in every voxel of any SR 3D volume estimated at time TE. T2 maps are computed using a non-linear least-squares optimization (MATLAB, MathWorks, R2019a) (see Figure 1-B). Please note that the T2 signal decay shows an offset between the first echoes and the remaining curve. This is an effect related to stimulated echoes [16] and to the sampling order of the HASTE sequence. It is common practice to exclude from the fitting the first points that exhibit the pure spin echo without the stimulated echo contributions as in the consecutive echoes.

2.2 Validation study

Quantitative phantom - Our validation is based on the system standard model 130 that was established by the National Institute for Standards and Technology (NIST) of the United States in collaboration with the International Society for Magnetic Resonance in Medicine (ISMRM). It is produced by QalibreMD (Boulder, CO, USA) and is hereafter referred to as the NIST phantom [12]. This quantitative phantom was originally developed to assess the repeatability and reproducibility of MRI protocols across vendors and sites. Our study focuses on a region-of-interest (ROI) represented by a blue square in Figure 1-A. It is centered on elements of the NIST phantom that have relaxometry properties close to those reported in the literature for *in vivo* brain tissue of fetuses and preterm newborns at 1.5 T [25, 24, 3, 10, 18], namely T2 values higher than 170 ms and 230 ms in grey matter and white matter respectively, and high T1 values. Accordingly, we focus on the following areas: (a) T2=428.3 ms, (b) T2=258.4 ms

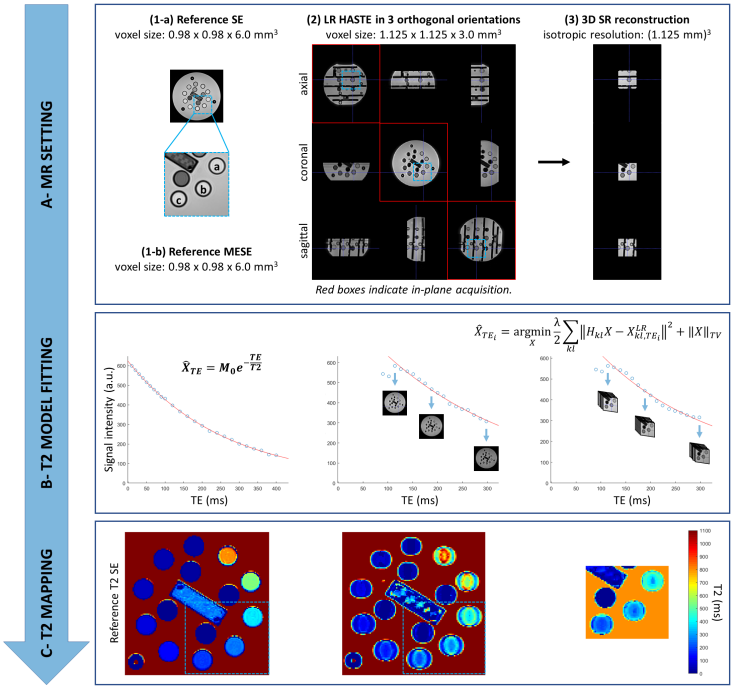

Fig. 1. Evaluation framework of the proposed 3D SR T2 mapping technique. Reference T2 values of elements (a), (b) and (c) (blue dashed area) of the NIST phantom are measured by (A-1-a) single-echo spin echo (SE) and (A-1-b) multi-echo spin echo (MESE) sequences. (A-2) Fast low-resolution orthogonal HASTE images acquired at variable TE are SR-reconstructed into (A-3) an isotropic HR volume for every TE. (B) The signal decay measured as a function of TE within every voxel of the images is fitted by a mono-exponential model. (C) Resulting voxel-wise T2 maps.

and (c) T2=186.1 ms, with a relatively high T1/T2 ratio (4.5-6.9), and which fall within a field-of-view similar to that of fetal MRI.

MR imaging - Acquisitions are performed at 1.5 T (MAGNETOM Sola, Siemens Healthcare, Erlangen, Germany), with an 18-channel body coil and a 32-channel spine coil (12 elements used). Three clinical T2w series of 2D thick slices are acquired in three orthogonal orientations using an ultra-fast multi-slice HASTE sequence (TE=90ms, TR=1200ms, excitation/refocusing pulse flip angles of 90°/180°, interslice gap of 10%, voxel size of $1.13 \times 1.13 \times 3.00mm^3$). For consistency with the clinical fetal protocol, a limited field-of-view (360 x 360mm^2) is imaged centered on the above-referenced ROI. A single series contains 23 slices to cover the defined ROI and is acquired in 28 seconds. Our study is performed with three orthogonal stacks only, thus, the acquisition time per TE is about 90

seconds. Binary masks are drawn on each LR series for reconstruction of a SR at every TE, as illustrated in Figure 1-3.

We extend the TE of this clinical protocol in order to acquire additional sets of three orthogonal series, leading to six configurations with 4, 5, 6, 8, 10, or 18 TEs uniformly sampled over the range of 90 ms to 298 ms. Therefore, the total acquisition time ranges from 6 minutes (4 TEs) to 26 minutes (18 TEs).

Gold-standard sequences for T2 mapping - A conventional single-echo spin echo (SE) sequence with variable TE is used as a reference for validation (TR=5000ms, 25 TEs sampled from 10 to 400ms, voxel size of $0.98 \times 0.98 \times 6.00mm^3$). One single 2D slice is imaged in 17.47 minutes for a given TE, which corresponds to a total acquisition time of more than 7 hours. According to the recommendations of the phantom manufacturer, an alternative multi-echo spin echo (MESE) sequence is used for comparison purposes (TR=5000ms, 32 TEs equally sampled from 13 to 416ms, voxel size of $0.98 \times 0.98 \times 6.00mm^3$). The acquisition time to image the same 2D slice is 16.05 minutes. All reference images and part of the HASTE data are made publicly available in the repository [14] for further reproducibility and validation studies.

Evaluation procedure - We evaluate the accuracy of our proposed 3D SR T2 mapping framework with regard to T2 maps obtained from HASTE, MESE and SE acquisitions. Since only one single 2D coronal slice is imaged by SE and MESE sequences, quantitative measures are computed on the corresponding slice of the coronal 2D HASTE series and 3D SR images.

At a voxel-wise level, T2 standard deviation and R^2 are computed to evaluate the fitting quality. A region-wise analysis is conducted over the three ROIs previously denoted as (a), (b) and (c). Automated segmentation of those areas is performed using the Hough transform in the original HASTE and SR images. An additional 1-pixel margin is applied to the minimal radius of the detected circles. Mean T2 values ($\pm$ standard deviation) are estimated within each ROI. The relative error in T2 estimation is computed using SE measurements as reference values. It is defined as the difference in T2 measures between either LR HASTE or SR and the corresponding SE reference value normalized by the SE reference value. This metric is used to evaluate the accuracy of our SR T2 mapping technique as well as its robustness in the presence of noise (see also Supplementary Material, Table 1).

We run the same MRI protocol (SE, MESE and HASTE) on three different days in order to study the repeatability of T2 measurements. The relative difference in T2 estimation between two independent experiments (i.e., on different days) is calculated as described above, using every measure in turn as a reference. Thus, we are able to evaluate the mean absolute percentage error $|\Delta\varepsilon|$ as the average of relative absolute errors in T2 estimation over all possible reference days.

3 Results

3.1 3D SR T2 mapping

T2 maps as derived from one coronal HASTE series and from 3D SR reconstruction of three orthogonal HASTE series are shown in Figure 2 together with voxel-wise associated T2 standard deviation maps. HASTE series show Gibbs ringing in the phase-encoding direction at the interface of the different elements. Since SE and MESE images are corrupted in a similar way across all TEs, a homogeneous T2 map is recovered for every element of the phantom (Figure 2). Instead, as HASTE acquisitions rely on a variable k-space sampling for every TE, resulting T2 maps are subject to uncompensated Gibbs artifacts that cannot easily be corrected due to reconstruction of HASTE images by partial Fourier techniques [13]. Interestingly though, Gibbs ringing is much less pronounced in the SR reconstructions where it is probably attenuated by the combination of orthogonal series. Of note, *in vivo* data are much less prone to this artifact.

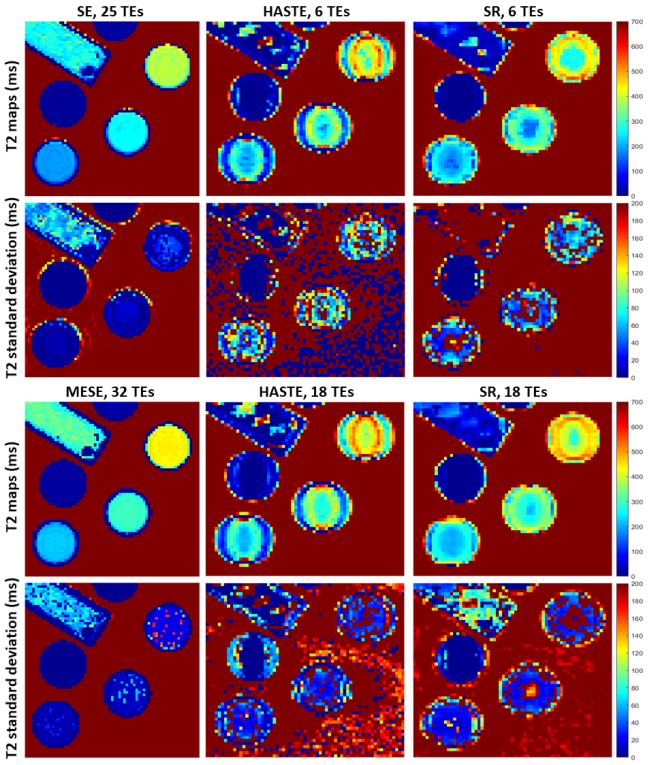

Fig. 2. Comparison of voxel-wise T2 maps and standard deviation maps estimated from SE, MESE, HASTE and corresponding SR reconstructions with multiple TEs.

3.2 Repeatability study

T2 estimation is highly repeatable over independent measurements with a mean absolute percentage error of less than 5% in LR HASTE images, respectively 10% in corresponding SR reconstructions (Table 1). The maximum variation is less than 4%, respectively 8%, of the measured T2 value for HASTE acquisitions and SR with 5 TEs.

Table 1. Repeatability of T2 mapping strategies between three independent experiments. Mean fitted T2 value ± standard deviation, coefficient of variation (CV), mean absolute difference ($|\Delta$T2$|$) and mean absolute percentage error ($|\Delta\varepsilon|$) in T2 estimation are presented. The lowest differences for each (ROI, method) pair are shown in bold.

		SE	MESE	HASTE/SR					
TEs		25	32	4	5	6	8	10	18
T2(ms)	(a)	380±7	435±4	422±2/288±7	427±12/312±21	425±2/352±13	451±4/409±18	454±0/403±20	451±2/407±12
	(b)	256±5	295±2	314±6/188±8	304±12/223±11	315±4/258±5	337±6/287±8	335±9/288±4	333±10/297±4
	(c)	187±2	217±2	252±9/159±10	247±2/180±14	249±4/207±6	267±1/225±5	267±6/223±4	263±3/233±4
CV(%)	(a)	1.8	1.0	0.4/**2.3**	2.8/6.7	0.5/3.8	1.0/4.4	**0.0**/5.0	0.4/3.0
	(b)	1.8	0.8	1.8/4.4	3.9/4.8	**1.3**/2.0	1.8/2.9	2.8/1.6	2.9/**1.2**
	(c)	1.0	0.7	3.6/6.2	0.8/7.7	1.5/2.9	**0.3**/2.4	2.2/**1.7**	1.1/1.9
$\|\Delta$T2$\|$(ms)	(a)	9.1	5.7	1.9/**8.9**	15.8/24.4	2.7/17.8	5.2/23.3	**0.2**/26.8	2.6/15.4
	(b)	6.1	3.2	7.7/11.1	14.2/13.8	**4.9**/6.0	7.7/10.8	11.4/5.6	12.8/**4.2**
	(c)	2.1	2.0	12.1/11.8	2.6/16.4	4.5/7.7	**1.1**/7.2	6.9/**4.9**	3.8/5.3
$\|\Delta\varepsilon\|$(%)	(a)	2.4	1.3	0.4/**3.1**	3.7/7.7	0.6/5.1	1.2/5.7	**0.0**/6.7	0.6/3.8
	(b)	2.4	1.1	2.4/5.9	4.6/6.3	**1.6**/2.3	2.3/3.8	3.4/1.9	3.9/**1.4**
	(c)	1.1	0.9	4.8/7.3	1.1/9.4	1.8/3.7	**0.4**/3.2	2.6/**2.2**	1.4/2.3

3.3 Impact of the number of TEs on T2 measurements

In an effort to optimize the acquisition scheme, especially regarding SAR deposition and reasonable acquisition time in a context of fetal examination, we investigate the influence of the number of TEs on the T2 estimation accuracy. Since T2 measurements are found highly repeatable throughout independent experiments, we arbitrarily select the measurements obtained on one day to perform this accuracy study.

T2 estimation by both clinical HASTE acquisitions and corresponding SR reconstructions demonstrate a high correlation with reference SE values over the 180-400 ms range of interest (see Figure 1 in Supplementary Material). Bland-Altman plots (Figure 3) show that average HASTE-based T2 quantification errors are almost the same across all configurations, independently of the studied ROI. Conversely, SR-based quantification errors vary depending on the targeted T2 value. Overall, SR-based T2 mapping exhibits the smallest average difference for 6 TEs. Figure 4 displays the relative error in T2 quantification as compared to SE measurements according to the number of TEs acquired. MESE

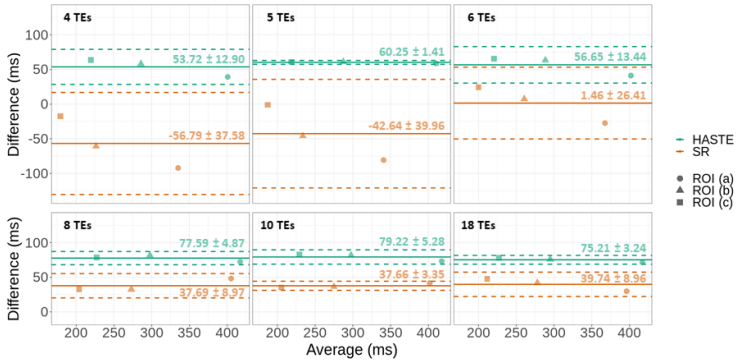

Fig. 3. Bland-Altman plots of differences in T2 quantification between HASTE from various numbers of TEs/corresponding SR reconstructions and reference SE in three ROIs.

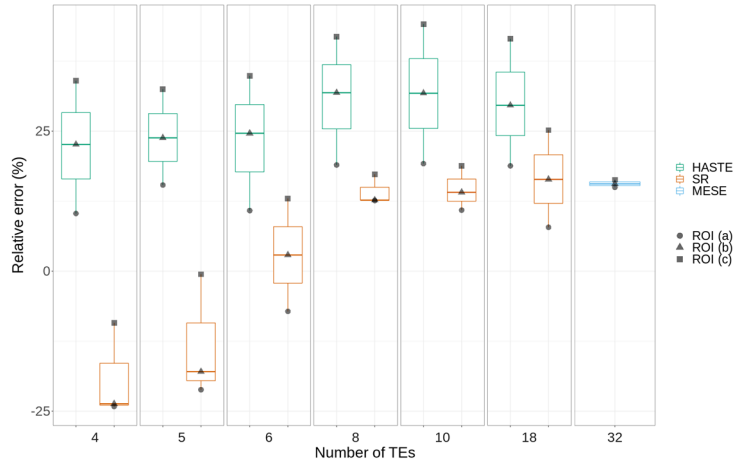

Fig. 4. Relative error in T2 quantification according to the method and number of TEs as compared to reference SE measurements.

provides T2 quantification with a small dispersion but with low out-of-plane resolution and prohibitive scanning times in a context of fetal MRI. In the following, its 16%-average relative error is considered an acceptable reference error level. HASTE-based T2 quantification overestimates T2 values in our range of interest by around 25%. As for MESE-based T2 mapping, such an overestimation can be attributed to stimulated echo contamination [16]. In the case of SR, the mean relative error in T2 quantification is less than 14%. However, the relative error in SR-based T2 measurement depends on the number of TEs acquired. Below 6 echoes, SR enables a dramatic improvement in T2 quantification over the HASTE-based technique, but only for T2 values less than 200 ms. Above

6 TEs, both SR and MESE have approximately the same average error. For 6 echoes, SR substantially outperforms HASTE and MESE over the whole range of T2 values studied with a relative error less than 11%. Furthermore, preliminary results on T2 quantification from HASTE images corrupted by higher levels of noise and their corresponding SR reconstructions in this optimized set-up using 6 echoes demonstrate the robustness of our SR T2 mapping technique (see Supplementary Material, Table 1). Overall, SR substantially outperforms HASTE for T2 quantification.

4 Conclusion

This work demonstrates the feasibility of repeatable, accurate and robust 3D isotropic HR T2 mapping based on SR-reconstructed clinical fast spin echo MR acquisitions. We have shown that SR-based T2 quantification performs accurately in the range of interest for fetal brain studies (180-430 ms) as compared with reference acquisitions such as SE and MESE. Thus, the proposed technique could provide 3D isotropic 1-mm^3 T2 maps of the fetal brain in a reasonable acquisition time. Moreover, it could be straightforwardly translated to the clinic since only the TE of the HASTE sequence routinely used in fetal exams needs to be adapted. A pilot study will be conducted on an adult brain to replicate these results *in vivo*. Although our study focuses on static data, the robustness of SR techniques to motion makes us hypothesize that 3D HR T2 mapping of the fetal brain is feasible. The number of TEs required for an accurate T2 quantification in this context has to be explored.

Acknowledgement. This work was supported by the Swiss National Science Foundation through grants 141283 and 182602, the Centre d'Imagerie BioMédicale (CIBM) of the UNIL, UNIGE, HUG, CHUV, EPFL as well as the Leenaards and Jeantet Foundations to Meritxell Bach Cuadra, and the Swiss Heart Foundation to Ruud B. van Heeswijk. The authors would like to thank Yasser Alemán-Gómez for his help in the rebuttal process.

References

1. Abd Almajeed, A., Adamsbaum, C., Langevin, F.: Myelin characterization of fetal brain with mono-point estimated T1-maps. Magnetic Resonance Imaging **22**(4), 565–572 (May 2004). https://doi.org/10/frdp45, 00009
2. Bano, W., Piredda, G.F., Davies, M., Marshall, I., Golbabaee, M., Meuli, R., Kober, T., Thiran, J.P., Hilbert, T.: Model-based super-resolution reconstruction of T2 maps. Magnetic Resonance in Medicine **83**(3), 906–919 (Mar 2020). https://doi.org/10/gf85n4, 00000
3. Blazejewska, A.I., Seshamani, S., McKown, S.K., Caucutt, J.S., Dighe, M., Gatenby, C., Studholme, C.: 3D in utero quantification of T2* relaxation times in human fetal brain tissues for age optimized structural and functional MRI. Magnetic Resonance in Medicine **78**(3), 909–916 (2017). https://doi.org/10/gf2n9z, 00000

4. Chen, L.W., Wang, S.T., Huang, C.C., Tu, Y.F., Tsai, Y.S.: T2 Relaxometry MRI Predicts Cerebral Palsy in Preterm Infants. American Journal of Neuroradiology **39**(3), 563–568 (Mar 2018). https://doi.org/10/gdcz66, http://www.ajnr.org/content/39/3/563, 00000 Publisher: American Journal of Neuroradiology Section: Pediatrics
5. Deoni, S.C.: Quantitative Relaxometry of the Brain. Topics in magnetic resonance imaging : TMRI **21**(2), 101–113 (Apr 2010). https://doi.org/10/fj3m42, https://www.ncbi.nlm.nih.gov/pmc/articles/PMC3613135/, 00152
6. Dingwall, N., Chalk, A., Martin, T.I., Scott, C.J., Semedo, C., Le, Q., Orasanu, E., Cardoso, J.M., Melbourne, A., Marlow, N., Ourselin, S.: T2 relaxometry in the extremely-preterm brain at adolescence. Magnetic Resonance Imaging **34**(4), 508–514 (May 2016). https://doi.org/10/ggb9qn, 00006
7. Ebner, M., Wang, G., Li, W., Aertsen, M., Patel, P.A., Aughwane, R., Melbourne, A., Doel, T., Dymarkowski, S., De Coppi, P., David, A.L., Deprest, J., Ourselin, S., Vercauteren, T.: An automated framework for localization, segmentation and super-resolution reconstruction of fetal brain MRI. NeuroImage **206**, 116324 (Feb 2020). https://doi.org/10/ggdnsm, 00000
8. Gholipour, A., Estroff, J.A., Barnewolt, C.E., Robertson, R.L., Grant, P.E., Gagoski, B., Warfield, S.K., Afacan, O., Connolly, S.A., Neil, J.J., Wolfberg, A., Mulkern, R.V.: Fetal MRI: A Technical Update with Educational Aspirations. Concepts in magnetic resonance. Part A, Bridging education and research **43**(6), 237–266 (Nov 2014). https://doi.org/10/gf4bc6, https://www.ncbi.nlm.nih.gov/pmc/articles/PMC4515352/, 00038
9. Gholipour, A., Estroff, J.A., Warfield, S.K.: Robust super-resolution volume reconstruction from slice acquisitions: application to fetal brain MRI. IEEE transactions on medical imaging **29**(10), 1739–1758 (Oct 2010). https://doi.org/10/b2xmdp, 00239
10. Hagmann, C.F., De Vita, E., Bainbridge, A., Gunny, R., Kapetanakis, A.B., Chong, W.K., Cady, E.B., Gadian, D.G., Robertson, N.J.: T2 at MR Imaging Is an Objective Quantitative Measure of Cerebral White Matter Signal Intensity Abnormality in Preterm Infants at Term-equivalent Age. Radiology **252**(1), 209–217 (Jul 2009). https://doi.org/10/bqkd9r, https://pubs.rsna.org/doi/10.1148/radiol.2522080589, 00048 Publisher: Radiological Society of North America
11. Kainz, B., Steinberger, M., Wein, W., Kuklisova-Murgasova, M., Malamateniou, C., Keraudren, K., Torsney-Weir, T., Rutherford, M., Aljabar, P., Hajnal, J.V., Rueckert, D.: Fast Volume Reconstruction From Motion Corrupted Stacks of 2D Slices. IEEE transactions on medical imaging **34**(9), 1901–1913 (Sep 2015). https://doi.org/10/f3svr5, 00089
12. Kathryn E Keenan , Karl F Stupic, Michael A Boss, Stephen E Russek, Tom L Chenevert, Pottumarthi V Prasad, Wilburn E Reddick, Kim M Cecil, Jie Zheng, Peng Hu, Edward F Jackson, and Ad Hoc Committee for Standards in Quantitative MR: Multi-site, multi-vendor comparison of T1 measurement using ISMRM/NIST system phantom. In: ISMRM Singapore Proceedings. vol. program number 3290. Singapore (2016), http://archive.ismrm.org/2016/3290.html, 00030
13. Kellner, E., Dhital, B., Kiselev, V.G., Reisert, M.: Gibbs-ringing artifact removal based on local subvoxel-shifts. Magnetic Resonance in Medicine **76**(5), 1574–1581 (2016). https://doi.org/10/f9f64r, https://onlinelibrary.wiley.com/doi/abs/10.1002/mrm.26054, 00191 _eprint: https://onlinelibrary.wiley.com/doi/pdf/10.1002/mrm.26054

14. Lajous, H., Ledoux, J.B., Hilbert, T., van Heeswijk, R.B., Bach Cuadra, M.: Dataset t2 mapping from super-resolution-reconstructed clinical fast spin echo magnetic resonance acquisitions (Oct 2020). https://doi.org/10.5281/zenodo.3931812, https://zenodo.org/deposit/3931812
15. Leppert, I.R., Almli, C.R., McKinstry, R.C., Mulkern, R.V., Pierpaoli, C., Rivkin, M.J., Pike, G.B., Brain Development Cooperative Group: T2 relaxometry of normal pediatric brain development. Journal of magnetic resonance imaging: JMRI **29**(2), 258–267 (Feb 2009). https://doi.org/10/c77mvm, 00000
16. McPhee, K.C., Wilman, A.H.: Limitations of skipping echoes for exponential T2 fitting. Journal of magnetic resonance imaging: JMRI **48**(5), 1432–1440 (2018). https://doi.org/10/ggdj43, 00004
17. Milford, D., Rosbach, N., Bendszus, M., Heiland, S.: Mono-Exponential Fitting in T2-Relaxometry: Relevance of Offset and First Echo. PLoS ONE **10**, e0145255 (Dec 2015). https://doi.org/10/gfc68d, 00036
18. Nossin-Manor, R., Card, D., Morris, D., Noormohamed, S., Shroff, M.M., Whyte, H.E., Taylor, M.J., Sled, J.G.: Quantitative MRI in the very preterm brain: assessing tissue organization and myelination using magnetization transfer, diffusion tensor and T1 imaging. NeuroImage **64**, 505–516 (Jan 2013). https://doi.org/10/f4jgtg, 00000
19. Rousseau, F., Kim, K., Studholme, C., Koob, M., Dietemann, J.L.: On super-resolution for fetal brain MRI. Medical image computing and computer-assisted intervention: MICCAI ... International Conference on Medical Image Computing and Computer-Assisted Intervention **13**(Pt 2), 355–362 (2010). https://doi.org/10/bns47p, 00069
20. Schneider, J., Kober, T., Bickle Graz, M., Meuli, R., Hüppi, P.S., Hagmann, P., Truttmann, A.C.: Evolution of T1 Relaxation, ADC, and Fractional Anisotropy during Early Brain Maturation: A Serial Imaging Study on Preterm Infants. AJNR. American journal of neuroradiology **37**(1), 155–162 (Jan 2016). https://doi.org/10/f7489d, 00025
21. Tourbier, S.: sebastientourbier/mialsuperresolutiontoolkit (May 2019), https://github.com/sebastientourbier/mialsuperresolutiontoolkit, 00000 original-date: 2017-03-16T15:22:13Z
22. Tourbier, S., Bresson, X., Hagmann, P., Thiran, J.P., Meuli, R., Bach Cuadra, M.: An Efficient Total Variation Algorithm for Super-Resolution in Fetal Brain MRI with Adaptive Regularization. NeuroImage **118** (Jun 2015). https://doi.org/10/f7p5zx, 00047
23. Travis, K.E., Castro, M.R.H., Berman, S., Dodson, C.K., Mezer, A.A., Ben-Shachar, M., Feldman, H.M.: More than myelin: Probing white matter differences in prematurity with quantitative T1 and diffusion MRI. NeuroImage. Clinical **22**, 101756 (2019). https://doi.org/10/ggnr3d, 00002
24. Vasylechko, S., Malamateniou, C., Nunes, R.G., Fox, M., Allsop, J., Rutherford, M., Rueckert, D., Hajnal, J.V.: T2* relaxometry of fetal brain at 1.5 Tesla using a motion tolerant method. Magnetic Resonance in Medicine **73**(5), 1795–1802 (May 2015). https://doi.org/10/gf2pbh, 00000
25. Yarnykh, V.L., Prihod'ko, I.Y., Savelov, A.A., Korostyshevskaya, A.M.: Quantitative Assessment of Normal Fetal Brain Myelination Using Fast Macromolecular Proton Fraction Mapping. American Journal of Neuroradiology **39**(7), 1341–1348 (Jul 2018). https://doi.org/10/gdv9nf, http://www.ajnr.org/content/39/7/1341, 00006 Publisher: American Journal of Neuroradiology Section: Pediatrics